Materials Research Bulletin 46 (2011) 815–819

Contents lists available at ScienceDirect

Materials Research Bulletin

journal homepage: www.elsevier.com/locate/matresbu

Comparative study of physical properties of vapor chopped and nonchopped Al_2O_3 thin films

Sikandar H. Tamboli [a], Vijaya Puri [b], R.K. Puri [a,*], R.B. Patil [c], Meng Fan Luo [c]

[a] Vacuum Techniques & Thin Film Laboratory, USIC, Shivaji University, Kolhapur 416004, India
[b] Department of Physics, Shivaji University, Kolhapur 416004, India
[c] Department of Physics, National Central University, Taiwan

ARTICLE INFO

Article history:
Received 13 October 2010
Received in revised form 12 February 2011
Accepted 17 February 2011
Available online 24 February 2011

Keywords:
A. Oxides
A. Thin films
D. Optical properties
D. Mechanical properties
D. Surface properties

ABSTRACT

Aluminium oxide being environmentally stable and having high transmittance is an interesting material for optoelectronics devices. Aluminium oxide thin films have been successfully deposited by hot water oxidation of vacuum evaporated aluminium thin films. The surface morphology, surface roughness, optical transmission, band gap, refractive index and intrinsic stress of Al_2O_3 thin films were studied. The cost effective vapor chopping technique was used. It was observed that, optical transmittance of vapor chopped Al_2O_3 thin film showed higher transmittance than the nonchopped film. The optical band gap of vapor chopped thin film was higher than the nonchopped Al_2O_3, whereas surface roughness and refractive index were lower due to vapor chopping.

1. Introduction

A combination of high dielectric constant, high thermal conductivity, wear resistance, mechanical strength, chemical inertness, good adhesion to glass substrate and transparency over wide wavelength range [1–5] makes Al_2O_3 thin film a leading candidate for optoelectronics and microelectronics devices. The refractive index (1.76) of these films is in the range suitable for optical waveguide purpose also [4,5]. The properties of deposited Al_2O_3 thin films depend on the deposition process and optimized parameters. Reduction in defects and void formation and improved surface morphology are the basic requirements for minimum optical signal loss in optical waveguides.

Number of methods have been reported for deposition of Al_2O_3 thin films such as reactive magnetron sputtering [3], ion beam assisted deposition [6], pulsed laser deposition [4], spray pyrolysis [2], chemical vapor deposition, electron beam evaporation [7], cathodic vacuum arc [1], etc. The crystal structure, refractive index and adhesion properties of electron beam deposited vapor chopped Al_2O_3 thin films have been reported by our group previously [7].

In this paper, we report the physical properties of Al_2O_3 thin films that have been prepared by using hot water oxidation of vacuum evaporated vapor chopped and nonchopped aluminium thin films. The effects of vapor chopping on optical transmittance, optical band gap, refractive index, surface morphology, surface roughness and optical signal transmission loss properties were investigated.

2. Experimental

Aluminium oxide thin films have been prepared by using hot water oxidation of vacuum evaporated vapor chopped and nonchopped aluminium thin films, deposited on glass substrates under a vacuum of 10^{-5} mbar. Pure aluminium wire (Balzers 99.99%) was used as the evaporation source. After the deposition of vapor chopped and nonchopped aluminium thin films by resistive heating, these aluminium thin films were oxidized by using hot water oxidation method [7]. Three thicknesses of the Al_2O_3 thin film 100, 200 and 300 nm were investigated. During hot water oxidation the formation of Al_2O_3 could be observed from the disappearance of mirror reflecting aluminium metal thin film and becoming transparent. The vapor chopping technique (VCT) consists of a chopper which is a circular aluminium metal sheet of 10 cm diameter having a V-cut (155°) shape. This thin circular vane was fixed to a light aluminium rod attached to a motor. The rate of chopping in this study was 6 rot/s. As the chopper rotated, the filaments were exposed to the substrates. The vane was at a height of 10.5 cm from the source. The distance between source

* Corresponding author. Tel.: +91 0231 2609245; fax: +91 0231 2691533.
E-mail addresses: sikandar.physics@gmail.com (S.H. Tamboli), vrp_phy@unishivaji.ac.in (V. Puri), rkp_usic@unishivaji.ac.in (R.K. Puri), rrahulpatil@gmail.com (R.B. Patil), mfl28@phy.ncu.edu.tw (M.F. Luo).

0025-5408/$ – see front matter
doi:10.1016/j.materresbull.2011.02.037

and substrate was 12.5 cm. As the chopper rotated, the filaments were exposed to the substrates [7–9].

The film thickness was as measured by Tolansky interferometric method. The structural analysis was carried out with a Philips diffractometer (Philips PW 3710) at 1.54056 Å. Surface morphology study was done by SEM (JSM-6360 JEOL, JAPAN). The surface roughness was measured by atomic force microscope (AFM). The optical transmittance spectra were measured in the wavelength range from 200 to 800 nm by using a spectrophotometer (U 2800, Hitachi, Japan). The refractive index of Al_2O_3 thin films was measured by spectrophotometric method. Optical signal transmission loss property was measured by using prism coupling method. The optical transmission loss measurement setup details have been given elsewhere [10]. He–Ne laser has been used in this. Laser beam consists spot size 150 μm and 45° angle of incident.

The intrinsic stress of the thin films was measured by interferometric method [11] which works on Newton's ring principle. In this method the substrates were soda lime cover slips of diameter 1.9 cm and 0.022 cm thickness. The stress was calculated by measuring the variation in diameter of Newton's ring before and after deposition. The intrinsic stress was measured by equation

$$S = \frac{Yh^2(K_x - K_y)}{6t(1-\upsilon)}$$

where Young's modulus $(Y) = 3.44 \times 10^{11}$, Poisson's ration $(\upsilon) = 0.22$, thin film thickness (t), $h = 0.022$ cm (substrate thickness), K_x, K_y are the slope difference of plot $n\lambda/2$ vs. radius Newton's ring of before and after deposition.

3. Results and discussion

3.1. Structural

Fig. 1 shows the X-ray diffraction patterns of the nonchopped and vapour chopped Al_2O_3 thin films. The dominant cubic (2 2 0), α-Al_2O_3 and (4 2 2) phase was observed (reference code: 00-079-1557). (6 2 0) plane orientation was observed in only VC Al_2O_3 thin films, it was absent in NC. It was observed that the peaks observed in vapour chopped films were more intense than those in nonchopped films. The increased intensity can be attributed to the improved crystallinity, i.e. vapour chopped films were more crystalline than the nonchopped thin films. The improved structural order can be attributed to the increases in film density. No characteristic peaks of impurity and other phases were observed. The XRD patterns did not show evidence of the presence of aluminium metal, indicating complete oxidation of aluminium metal thin films to aluminium oxide thin films.

3.2. Surface morphology

Fig. 2 shows the surface morphology of vapor chopped and nonchopped Al_2O_3 thin films. It is seen that, nonchopped Al_2O_3 thin films show highly porous fibril morphology, whereas vapor chopped Al_2O_3 thin film gives smooth, dense continuous morphology.

Fig. 3 shows the 2-dimensional and 3-dimensional atomic force micrographs of vapor chopped and nonchopped Al_2O_3 thin films. The surface roughness of vapor chopped thin film was lesser than the nonchopped Al_2O_3 thin film. The granular structured grains were observed in vapor chopped as well as nonchopped Al_2O_3 thin films. The grain size of nonchopped thin film was higher than the vapor chopped Al_2O_3. Vapor chopped thin film was found to be denser than the nonchopped Al_2O_3 thin film.

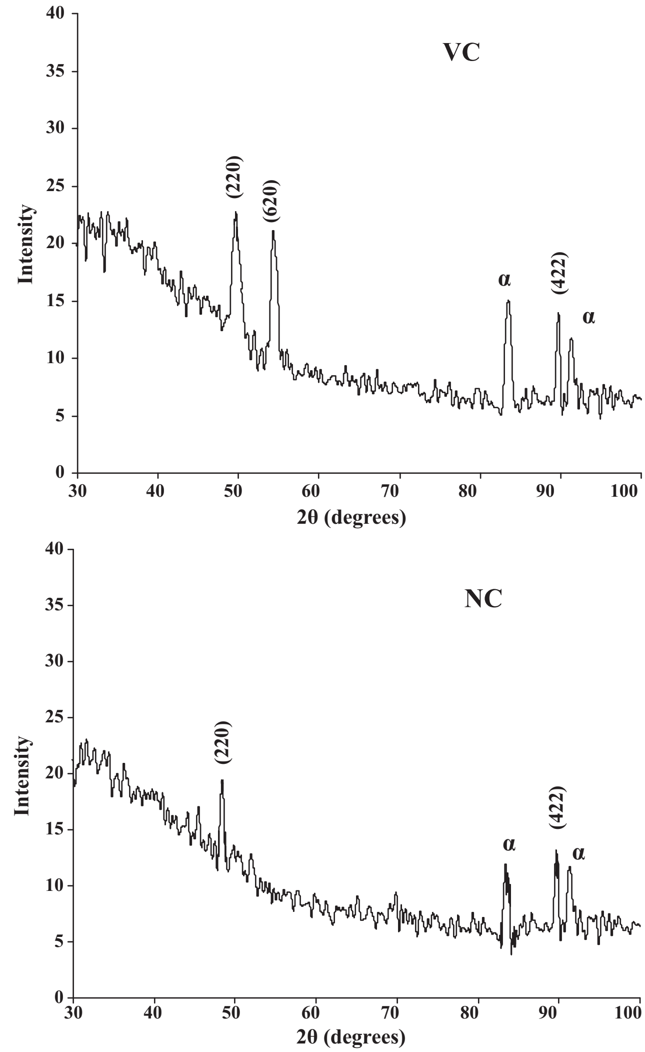

Fig. 1. XRD spectra of vapour chopped (VC) and nonchopped (NC) Al_2O_3 thin films.

3.3. Optical transmittance

Fig. 4 shows the optical transmittance of vapor chopped and nonchopped Al_2O_3 thin films of different thicknesses. The optical transmittance of vapor chopped and nonchopped thin films increased with the wavelength from 200 to 800 nm. It was observed that, optical transmittance decreased with increase in thin film thickness. Vapor chopped Al_2O_3 thin film showed higher optical transmittance than the nonchopped thin film. Vapor chopping produces better stoichiometry of the films, lesser defects and voids formation. The smaller grains in the vapor chopped thin film reduces the scattering losses at the grain boundaries whereby increasing the optical transmittance.

3.4. Optical band gap

Fig. 5 gives the graph of $(\alpha th\upsilon)^2$ as a function of $h\upsilon$ of Al_2O_3 thin films of 300 nm. From the absorption data, the band gap energy was calculated using formula:

$$\alpha = \frac{\alpha_0(h\upsilon - \mathrm{Eg})^n}{(h\upsilon)}$$

where 'Eg' is the separation between bottom of the conduction band and top of the valence band, α = absorption of thin film and

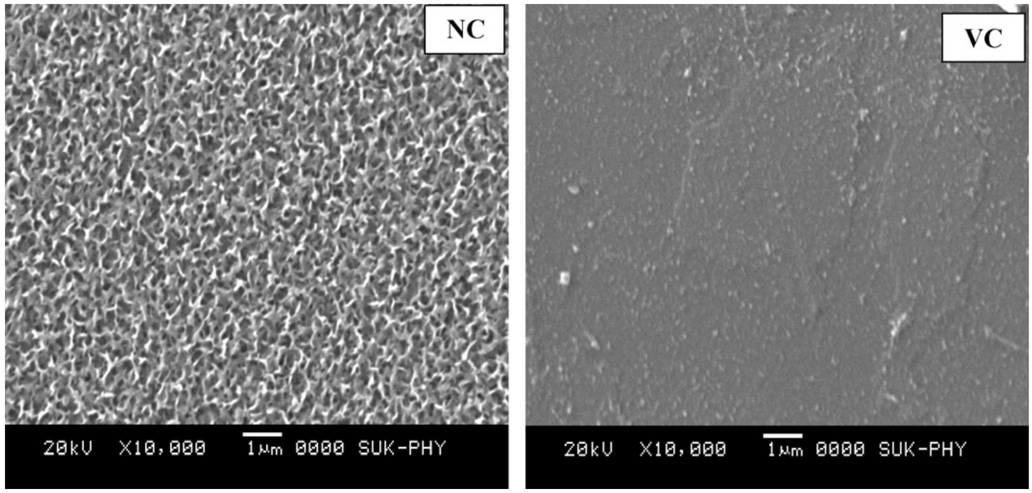

Fig. 2. Surface morphology of vapor chopped and nonchopped Al_2O_3 thin films.

α_0 = absorption coefficient, '$h\upsilon$' is the photon energy and 'n' is a constant. The value of n depends on the probability of transition; it takes values as 1/2, 3/2, 2 and 3 for direct allowed, direct forbidden, indirect allowed and indirect forbidden transition respectively.

Table 1 shows the optical band gap of vapor chopped and nonchopped Al_2O_3 thin films for different thicknesses. It was observed that, band gap increases with increase in thin film thickness. The band gap of nonchopped film was lesser than those of vapor chopped thin film. The lower observed band gap energies of nonchopped Al_2O_3 film might be due to varied extent of non-stoichiometry of the deposited layers, which may be due to the various lattice associated atomic interaction phenomena

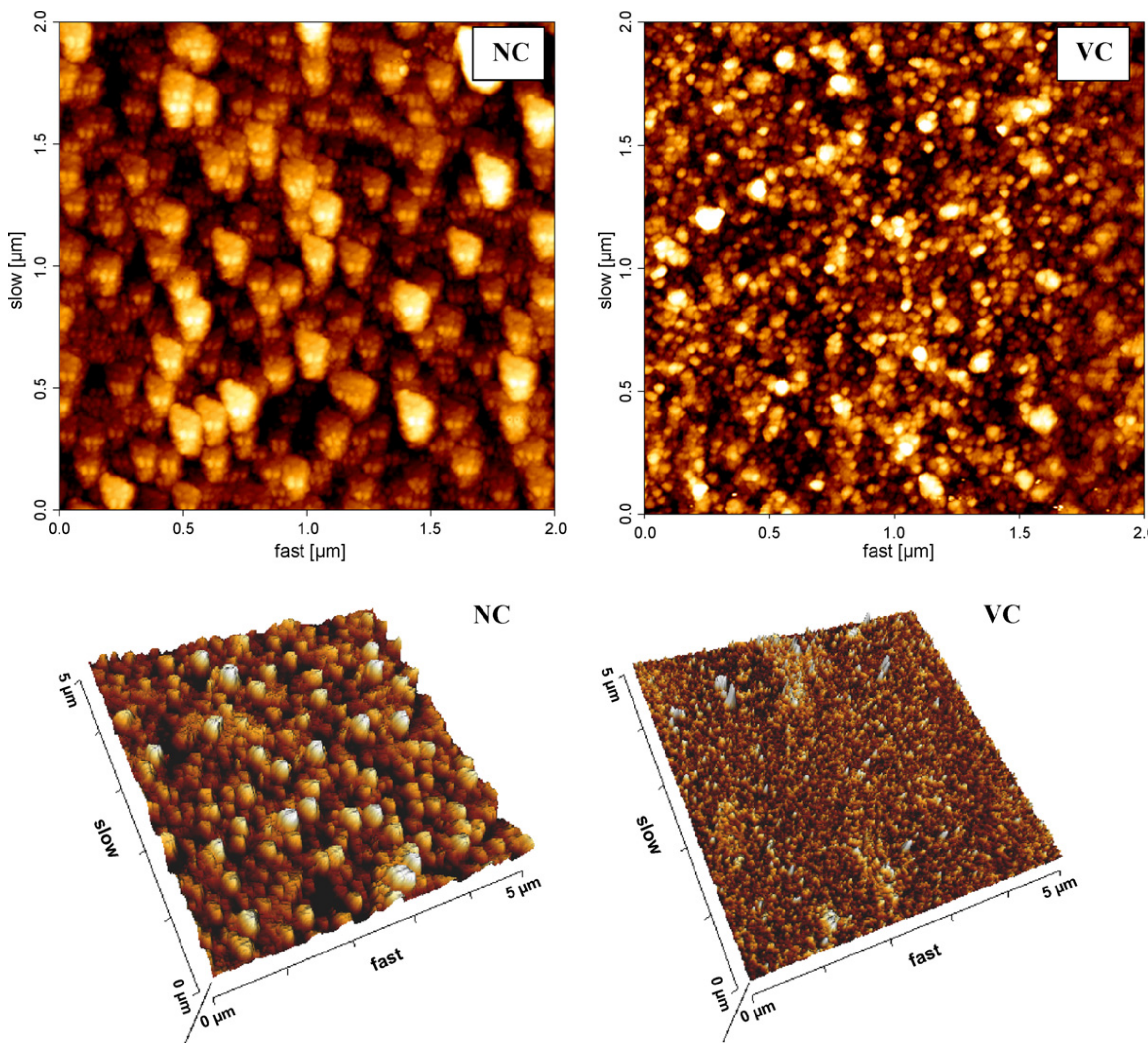

Fig. 3. 2-dimensional and 3-dimensional atomic force micrographs of vapor chopped (VC) and nonchopped (NC) Al_2O_3 thin films.

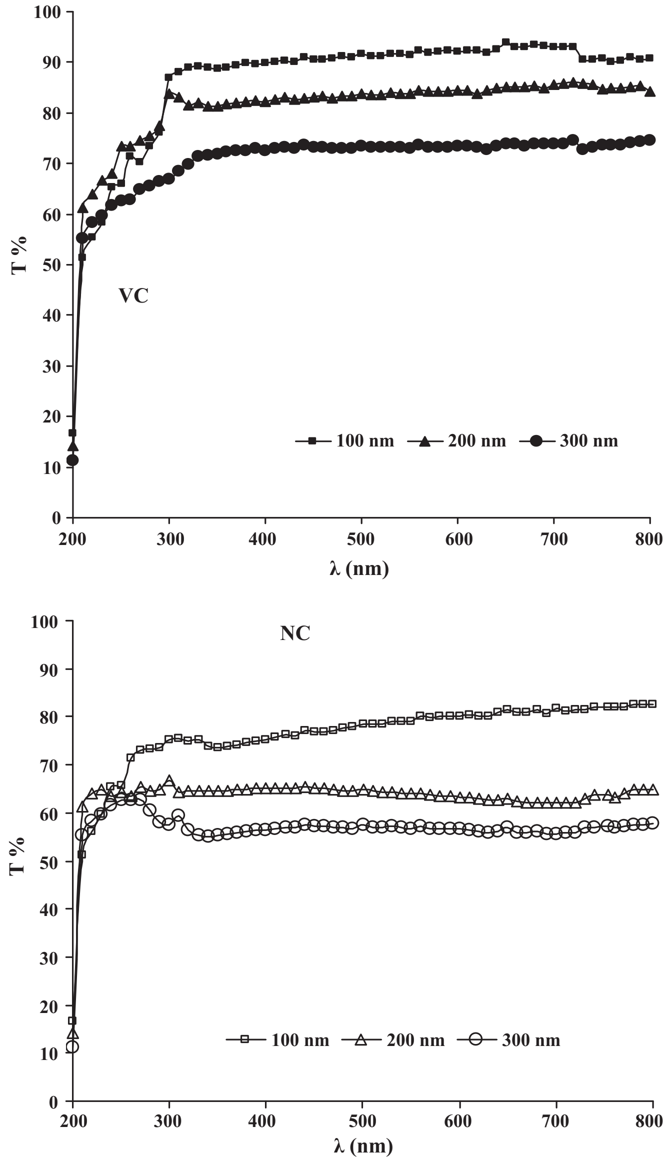

Fig. 4. Optical transmittance spectra of vapor chopped and nonchopped Al_2O_3 thin films.

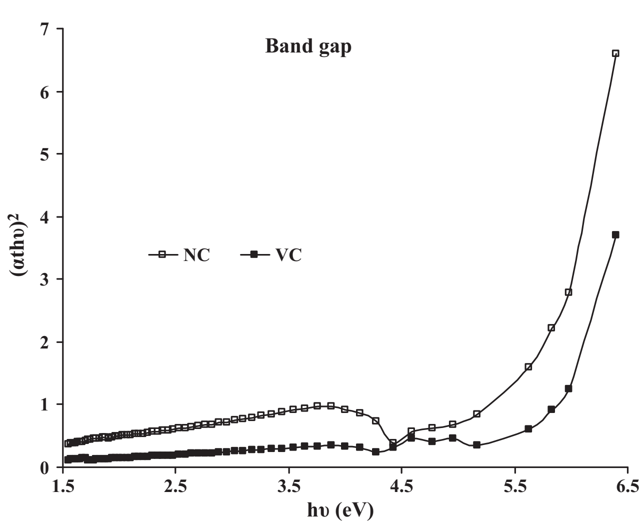

Fig. 5. $(\alpha th\upsilon)^2$ against $h\upsilon$ for vapor chopped and nonchopped Al_2O_3 thin films.

Table 1
Optical band gap and refractive index of vapor chopped and nonchopped Al_2O_3 thin films for different thin film thickness.

Thin film thickness (nm)	Optical band gap (eV)		Refractive index	
	NC	VC	NC	VC
100	4.5	4.7	1.63	1.59
200	5	5.3	1.66	1.62
300	5.6	5.8	1.69	1.66

coming into play due to the ionic crystalline nature. The band gap values obtained by us are in the reported range [12,13] and lesser than band gap of bulk aluminium oxide [14].

The lesser values of band gap of nonchopped film than vapor chopped film might also be due to the presence of more oxygen vacancies or due to defect related absorption or mobility gap of the more amorphous films. This induces change in the electronic structure of surfaces leading to a reduction in the ionic gap and in turn its total band gap [9].

During the evaporation process, the solid material turns to vapour form. The evaporated atoms (adatoms) acquires the kinetic energy, these adatoms may or may not be completely thermally equilibrated. When adatoms reaches nearer to the substrate, due to their different diffusion coefficient, adatoms moves horizontally over the substrate surface by jumping from one potential well to the other [15,16], it depends on adsorption residence time, adatoms nucleation rate and thermal activation energy of adatoms. In this adsorption residence time, the adatoms may interact with other adatoms to form a stable cluster. This adsorption residence time depends on various parameters such as binding energy between two adatoms, nucleation formation and their growth, material evaporation rate, density of adatoms, vapor pressure, etc. [15,16].

VCT interrupts the vapour flow during the adatoms condensation process before the condensation on the substrate with constant rate which give more residence time to the previously evaporated adatoms to settle completely at minimum energy potential well. This helps to create new nucleation centers and helps to minimize the columnar growth and form a uniform dense thin film. Adatoms nucleation density and nucleation rate become lesser which provides lesser defects and higher mobility of small cluster which reduces the defect formation. It is seen that if all the stable adatom pairs move quickly to join pre-existing larger clusters, then there will be a major suppression of the nucleation rate [16].

In vapour chopping technique, vapour chopper interrupt with 6 rot/s speed the evaporated material's vapour flow, block some evaporated adatoms and give more residential time for adatoms condensation on substrate. Same thickness of VC and NC Al_2O_3 thin film was maintained by providing more time for vapor chopped thin film deposition than nonchopped film.

3.5. Refractive index

The analytical method have been used for the calculation of refractive index n using the following formula [17]:

$$n = \left[\frac{n_s^2 T_f + n_s (1 + \sqrt{R_f})^2}{T_f + n_s (1 - \sqrt{R_f})^2} \right]^{1/2}$$

where n = refractive index of the film, n_s = refractive index of the substrate, T_f = transmittance of the film, R_f = reflectance of the film.

The refractive index values of nonchopped and vapour chopped aluminium oxide thin films for different thicknesses calculated at

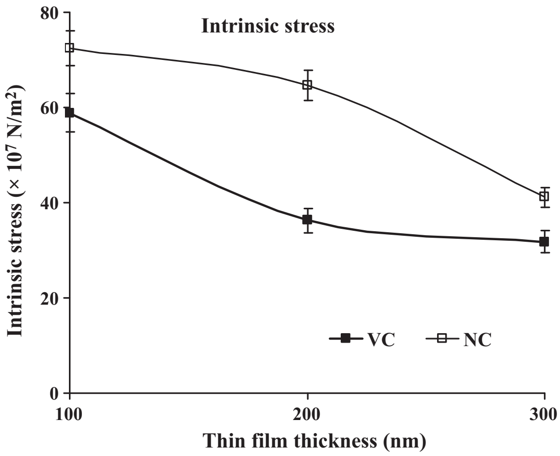

Fig. 6. Intrinsic stress of vapor chopped and nonchopped Al_2O_3 thin film for different thin film thickness.

590 nm are tabulated in Table 1. It was observed that, refractive index of VC and NC increased with increase in thin film thickness whereas it decreased due to vapor chopping. The refractive indices for vapor chopped thin films were in between 1.59 and 1.66 range whereas it was 1.63–1.69 for nonchopped thin films. These values are in the range reported [14,12].

3.6. Intrinsic stress

Fig. 6 shows the intrinsic stress of vapor chopped and nonchopped thin films for various thin film thickness. It was observed that, the intrinsic stress of vapor chopped and nonchopped Al_2O_3 thin films decreased with increase in thin film thickness. The vapor chopped thin films showed lesser intrinsic stress than the nonchopped Al_2O_3 thin film for all thicknesses. The intrinsic stress was tensile in nature.

Stress is related to crystal disorder, dislocations, voids [18] and density of thin films [19]. Vapor chopping technique helps to improve crystallinity and density of film and decrease in crystallite size, lattice disorder and voids in thin films resulting in decrease in intrinsic stress. At lower densities the stress distribution at the interface is sufficient to deform individual particles and affect the increment in intrinsic stress [18]. The dense vapor chopped Al_2O_3 thin film with less voids showed lesser intrinsic stress than nonchopped thin films. The voids and pores in nonchopped thin film is higher than in the vapor chopped thin film. Increase in porosity of the thin film causes an increase in stress.

3.7. Optical transmission loss

The optical transmission loss study of Al_2O_3 thin film waveguide of thickness 300 nm showed that, optical transmission loss of vapor chopped thin film (3.73 dB/cm) was lesser than the nonchopped Al_2O_3 (6.01 dB/cm). The optical transmission loss values of both VC and NC thin films were lesser than those reported (10 dB/cm) by Kersten et al. [5]. The effect of thin film thickness variations, i.e. 100, 200 and 300 nm was negligible ~0.5–0.8 dB/cm. The input optical beam scattering from the surface of thin film as it passes through the guiding structure is a root cause of optical signal transmission loss. Scattering of the beam occurs during the interaction of beam and thin film surface. AFM data clearly shows that, the vapor chopping technique gives smoother Al_2O_3 films than the nonchopped films. Surface roughness might be a reason of scattering of optical signal. Vacuum evaporated dielectric films grow as columnar structure with voids in between which causes density fluctuations. These columnar internal structures strongly scatter light. Even the grain boundaries and inhomogeneity in the grain boundaries also scatter light. In most of these films the grain size was of the order of magnitude of wavelength. Due to the vapor chopping technique films grow with smaller grain size, lesser defects, lesser voids, etc. causing lower scattering in these films. The improved surface morphology and reduced columnar structure, cracks and voids formation of MgO thin films by using vapor chopping technique observed by taking cross section SEM were reported in our earlier report [20]. The optical transmission loss of the vapor chopped aluminium oxide thin film waveguide being lesser than that of nonchopped waveguide is due to the combined effect of all the above processes. The more homogeneous nucleation occurring in the vapor chopped films might be reducing the reflection losses in the waveguide. The scattering losses due to the irregularities at the film surface or interface and also due to density fluctuations in the film are reduced due to vapor chopping.

4. Conclusion

Highly transparent aluminium oxide thin films were successfully deposited by hot water oxidized vacuum evaporated vapor chopped and nonchopped Al thin films. The cost effective vapor chopping technique has been found to modify the surface morphology and increase the optical transmittance, band gap with decrease in surface roughness and optical transmission loss of the Al_2O_3 thin films. Thicknesses variation also affects the optical transmittance, band gap, stress and refractive index whereas it has very negligible effect on optical transmission loss. Vapor chopping technique gives better quality and low scattering losses in optical waveguiding applications which may open a new window in the cutting edge research in this field.

Acknowledgements

Mr. Sikandar H. Tamboli is thankful to Shivaji University, Kolhapur for Departmental Research Fellowship (DRF). Vijaya Puri acknowledges Research Scientists (C) award from University Grants Commission (U.G.C.), India.

References

[1] Z.W. Zhao, B.K. Tay, G.Q. Yu, D.H.C. Chua, S.P. Lau, L.K. Cheah, Thin Solid Films 447–448 (2004) 14.
[2] M. Aguilar-Frutis, M. Garcia, C. Falcony, G. Plesch, S. Jimenez-Sandoval, Thin Solid Films 389 (2001) 200.
[3] K. Koski, J. Holsa, P. Juliet, Thin Solid Films 339 (1999) 240.
[4] A. Pillonnet, C. Champeaux, C. Bovier, R. Brenier, H. Jaffrezic, J. Mugnier, Appl. Phys. A 69 (1999) 735.
[5] R.T. Kersten, H.F. Mahlein, W. Rauscher, Thin Solid Films 28 (1975) 369.
[6] Q.Y. Zhang, W.J. Zhao, P.S. Wang, L. Wang, J.J. Xu, P.K. Chu, Nucl. Instrum. Meth. Res. B 206 (2003) 357.
[7] P.V. Patil, D.M. Bendale, R.K. Puri, Vijaya Puri, Thin Solid Films 288 (1996) 120.
[8] R.B. Patil, R.K. Puri, Vijaya Puri, Mater. Lett. 62 (2008) 198.
[9] S.H. Tamboli, R.B. Patil, S.V. Kamat, R.K. Puri, Vijaya Puri, J. Alloys Compd. 477 (2009) 855.
[10] P.V. Patil, R.K. Puri, Vijaya Puri, J. Opt. 27 (1998) 33.
[11] R.B. Patil, R.K. Puri, Vijaya Puri, J. Phys. Conf. Ser. 114 (2008) 012036.
[12] K.S. Shamala, L.C.S. Murthy, K.N. Rao, Mater. Sci. Eng. B 106 (2004) 269.
[13] S.D. Mo, W.Y. Ching, Phys. Rev. B 57 (1997) 15297.
[14] M. Schmid, M. Shishkin, G. Kresse, E. Napetschnig, P. Varga, M. Kulawik, N. Nilius, H.P. Rust, H.J. Freund, Phys. Rev. Lett. 97 (2006) 046101.
[15] K.L. Chopra, Thin film Phenomena, McGraw-Hill, New York, 1969.
[16] J.A. Venables, Surf. Sci. 299/300 (1994) 798.
[17] Y. Zheng, K. Kikuchi, Appl. Opt. 36 (1997) 25.
[18] R. Koch, D. Winau, K.H. Rieder, Phys. Scripta T49 (1993) 539.
[19] A.K. Sinha, H.J. Levinstrin, T.E. Smith, J. Appl. Phys. 49 (4) (1978) 2423.
[20] S.H. Tamboli, Vijaya Puri, R.K. Puri, J. Alloys Compd. 503 (2010) 224.